

Damage Identification by the Dynamic Virtual Distortion Method
(excerpt of the article in the J. Intelligent Material Systems & Structures,
vol. 15, issue 6, pp. 479-494)

Przemysław Kołakowski, Tomasz G. Zieliński, Jan Holnicki-Szulc
Institute of Fundamental Technological Research
Polish Academy of Sciences
SMART-TECH Centre
Swietokrzyska 21, 00-049 Warsaw, Poland
e-mails: pkolak@ippt.gov.pl, tzielins@ippt.gov.pl, holnicki@ippt.gov.pl

Key words:

Damage identification, inverse dynamic analysis, elastic wave propagation

Abstract

This paper presents a novel approach to damage identification based on the phenomenon of elastic waves propagation. The theoretical background is the dynamic Virtual Distortion Method, which is capable of modelling both a reference excitation signal propagated in the structure over a time domain and a perturbed signal due to damaged locations. The related methodology is presented including a brief description of experimental verification. Numerical example with successful, multi-damage case identification is demonstrated. Advantages of the approach as well as its challenging points are discussed.

1 Introduction

Our purpose in this paper is to propose a novel approach to the inverse dynamic analysis problem making use of the phenomenon of elastic wave propagation in engineering structures.

Generalising the VDM approach for dynamic problems, a time-dependent influence matrix D is defined, describing structural response to locally generated unit impulses. Pre-computation of the time-dependent matrix D allows for decomposition of the global dynamic structural response into components caused by external excitation in undamaged structure and components describing perturbations caused by internal defects.

The proposed, time-domain-based methodology of data processing for damage identification (*VDM software*) fits well to the following scheme of measurements:

- i) wave generator produces a low frequency impulse (e.g. of sine shape, 1-10 ms period), close to a resonance frequency, providing long-distance propagation of elastic wave,
- ii) few, well-located, distant sensors collect measurements of frontal part of the generated wave,
- iii) if the received structural response differs significantly from the reference response (of undamaged structure), the collected measurements are transmitted to a computer centre for further data processing (VDM-based damage identification).

2 Dynamic influence matrix

We will be dealing with dynamic analysis, so we need to introduce a time factor into the VDM.

Any form of dynamic excitation can be composed from series of short impulses (see Fig. 2.2). So we calculate influence matrix as a 3-dimensional matrix of dynamic responses obtained for unit impulse excitations applied in the time instant $t=0$ (Fig. 2.3a). It is important to notice that we can simulate this impulse load by applying initial velocity conditions in Newmark's integration. Having calculated all the columns of the influence matrix D_{ij} , which gathers the dynamic response for impulse excitations imposed in time instant $t=0$, it appears that we should compute the following matrices as well for the impulse excitations applied in the successive time instants τ (Fig. 2.3b). Fortunately, we do not need to do that, thanks to the following, obvious relationship:

$$D_{ij}^{\tau}(t) = \begin{cases} 0 & \text{for } t < \tau \\ D_{ij}(t - \tau) & \text{for } t \geq \tau \end{cases} \quad (2.16)$$

where D_{ij} is the already calculated dynamic influence matrix. So for all our further purposes we have only one time-dependent influence matrix computed for unit impulse excitation applied at the beginning of the assumed time period.

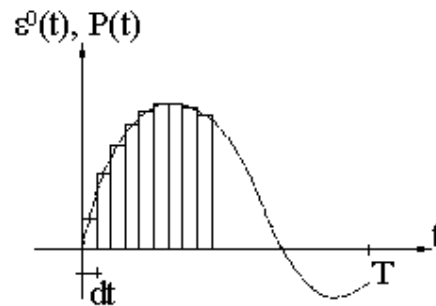


Fig. 2.2 Short impulses composing a dynamic excitation

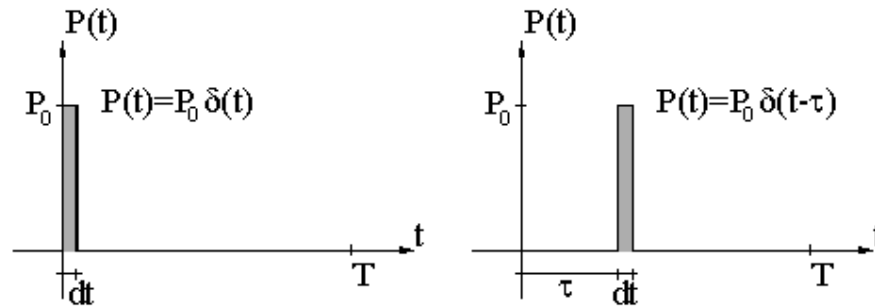


Fig. 2.3 Unit impulse excitation applied
a) at the beginning of the assumed time period
b) at an arbitrary time instant τ

3 Experimental check of concept feasibility

A 90 cm long, aluminium, cantilever beam with mounted piezo-wave generator (Fig. 3.1a) and piezo-sensor (Fig. 3.1b) was tested: i) as a healthy, intact structure producing a reference response and ii) as a damaged structure (perturbed response) affected by corrosion, modelled as a series of cuts in order to account for local stiffness change rather than mass change. The exciting full sine impulse of the period 0.007s was applied. The essence of the damage identification is to solve the inverse dynamic problem, which means introducing such modification to the beam model that the numerical curve fits the experimental curve in the best possible way. The result of the damage identification (utilising the experimental response) for the beam, discretised into 25 finite elements, is shown in Fig. 3.4. Let us note that the detected damage zone is spread over several finite elements including the really damaged ones.

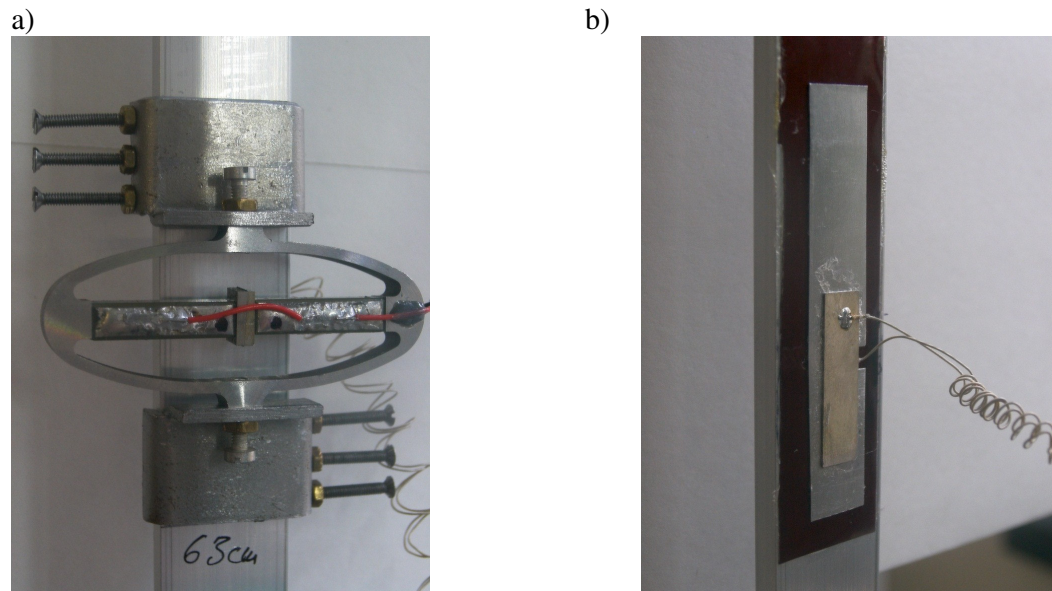


Fig. 3.1 Photos of the actuator (a) and the sensor (b) mounted on an aluminium beam

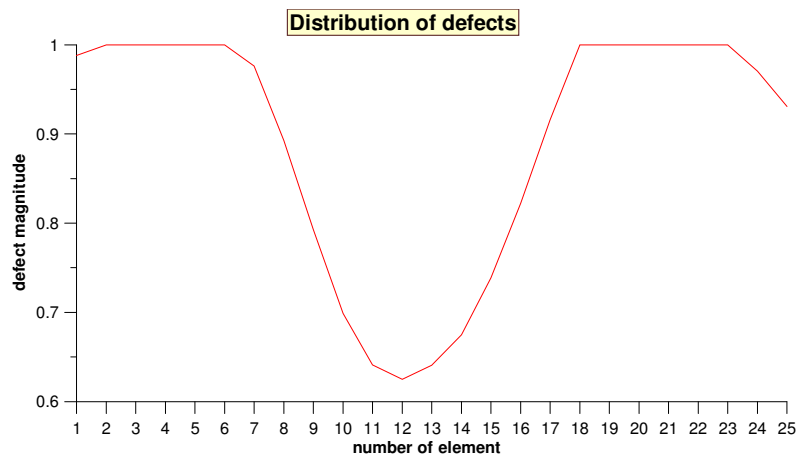


Fig. 3.4 Result of damage identification for the aluminium beam damaged in the middle part (real damage in element No. 12 and 13)

4 Dynamic approach to damage identification

4.1 VDM-based damage identification

4.1.1 Modelling of wave propagation

Let us describe the dynamic response of the strain increment $\Delta \varepsilon_A(t)$ in the location A and the time instance t as the superimposed response caused by impulses of the so-called *virtual distortion* increments $\Delta \varepsilon_\alpha^0(\tau)$ generated in the locations α and the time instances τ (cf. Fig. 4.1):

$$\Delta \varepsilon_A(t) = \sum_{\tau \leq t} \sum_{\alpha} D_{A\alpha}(t - \tau) \Delta \varepsilon_\alpha^0(\tau), \quad (4.1)$$

where the dynamic, time-dependent, influence matrix $D_{A\alpha}(t - \tau)$ describes the corresponding dynamic response of the strain in the location A and the time instance t , caused by the unit impulse virtual distortions forced in the locations α and the time instances $\tau \leq t$. Note that it is sufficient to compute only the matrix $D_{A\alpha}(t)$, which stores the response for the appropriate unit impulse distortion forced in the initial time instant $\tau = 0$. The virtual distortion increments $\Delta \varepsilon_\alpha^0(\tau)$ model excitations caused in locations α by the piezoelectric transducers. In the paper, we assume that small Greek subscripts (α) run through all locations of wave-generators while the capital Latin ones (A) run through locations of wave-receivers (sensors). The elements of the influence matrix $D_{A\alpha}(t)$ can be determined through the integration of the motion equations (e.g. using the Newmark's method) computed for the unit impulse excitation generated sequentially in the structural elements α . The unit impulse excitation can be introduced in the form of initial velocity conditions: $v(0) = P \Delta t / m$, where P denotes the so-called *compensative* force corresponding to locally generated unit virtual distortion impulse $\varepsilon^0 = 1$, Δt is the integration time step, and m is the mass concentrated in the charged node of the loaded structural element α . Assuming (for simplicity of presentation) a discrete model of a truss structure (Fig. 4.1), we can describe the transient function for the wave propagation generated in members α and received in member(s) A . To this end it is necessary to determine in advance, the time dependent dynamic influence matrix $D_{A\alpha}(t)$, where t runs through all time steps of the dynamic analysis: $t \in \langle 0, T \rangle$. Having the influence matrix computed, we can calculate the superposition (4.1), where $\Delta \varepsilon_\alpha^0(\tau)$ describes (for the sequence of τ instances) the shape of the excited signal. Then, we can achieve the form of the strain in location A and the time period $\langle 0, T \rangle$ by summing the strain increments for all successive time instances $t \in \langle 0, T \rangle$:

$$\varepsilon_A(t) = \sum_{\tau \leq t} \Delta \varepsilon_A(\tau) = \varepsilon_A(t-1) + \Delta \varepsilon_A(t) \quad (4.2)$$

In this way, the storage of the influence matrix $D_{A\alpha}(t)$, allows us to determine the transient function (between locations α and A) for any shape of the excited signal.

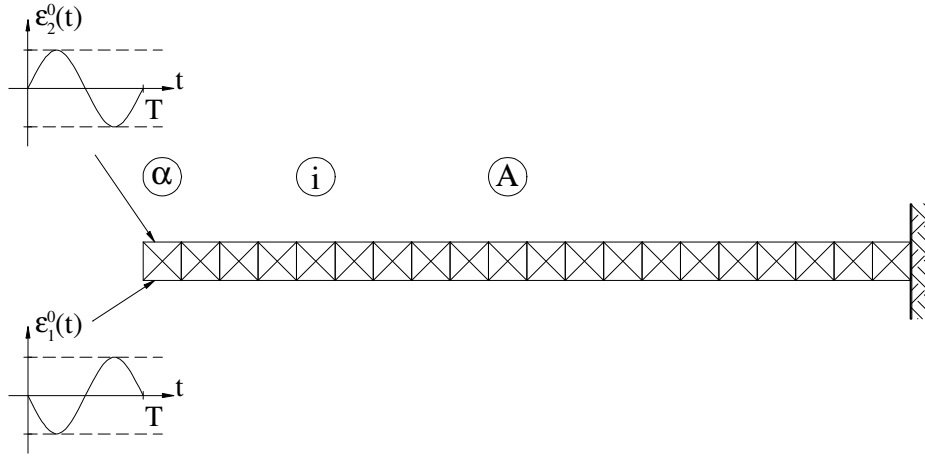


Fig. 4.1 Cantilever truss subject to piezo-excitation

4.1.2 Modelling of damage

Let us apply the above-described, influence matrix-based approach to the damage influence description. Three new, time-dependent, influence matrices ($D_{Ai}(t)$, $D_{i\alpha}(t)$, $D_{ij}(t)$) will be introduced. The method of computation of the matrices is similar to the one described in the previous chapter. In the case of any perturbation of elastic wave propagation caused by defects in structural members i (between the locations α of the wave generators and the location A of the wave receivers), it is necessary to generalise the formula (4.1) adding the component $\Delta\mathcal{E}_A^R(t)$ related to the perturbation caused by these defects:

$$\Delta\mathcal{E}_A(t) = \Delta\mathcal{E}_A^L(t) + \Delta\mathcal{E}_A^R(t) = \sum_{\tau \leq t} \left[\sum_{\alpha} D_{A\alpha}(t-\tau) \Delta\mathcal{E}_{\alpha}^0(\tau) + \sum_i D_{Ai}(t-\tau) \Delta\mathcal{E}_i^0(\tau) \right], \quad (4.3)$$

where $\Delta\mathcal{E}_A^L(t)$ is the part of the strain increment caused by virtual distortion increments $\Delta\mathcal{E}_{\alpha}^0(t)$ modelling piezoelectric excitations, whereas $\Delta\mathcal{E}_A^R(t)$ is the component caused by virtual distortion increments $\Delta\mathcal{E}_i^0(t)$ simulating defects. From now on, we assume that small Latin indices (i, j, k, l) run through all presumed locations of possible defects. The defect-simulating virtual distortion increment can be expressed by the following formula:

$$\Delta\mathcal{E}_i^0(t) = (1 - \mu_i) \Delta\mathcal{E}_i(t), \quad (4.4)$$

where $\mathcal{E}_i(t)$ denotes the strain in member i and the time instance t , while $\mu_i = E_i/E_i'$ denotes the ratio of the damaged member Young's modulus to the initial one. Therefore, the parameter $\mu_i \in \langle 0, 1 \rangle$ specifies the size of the defect in location i (actually $\mu_i = 1$ means that there is no damage, while $\mu_i = 0$ means that the member i is completely damaged so that it can sustain no stresses). If we assume several possible defect locations i (eventually, all structural elements of the structure), we can agree that the vector μ_i specifies also the distribution of these defects.

The above relation (6.4) comes from the more general formula:

$$\mu_i = \frac{E_i}{E'_i} = \frac{\varepsilon_i(t) - \varepsilon_i^0(t)}{\varepsilon_i(t)} = \frac{\Delta\varepsilon_i(t) - \Delta\varepsilon_i^0(t)}{\Delta\varepsilon_i(t)}, \quad (4.5)$$

in which virtual distortions simulate material parameter modifications (e.g. material redistribution $\mu_i = A_i/A'_i$). Now, let us express the strains $\Delta\varepsilon_i(t)$ in the formula (4.4) through the formula analogous to equation (4.3):

$$\Delta\varepsilon_i(t) = \Delta\varepsilon_i^L(t) + \Delta\varepsilon_i^R(t) = \sum_{\tau \leq t} \left[\sum_{\alpha} D_{i\alpha}(t-\tau) \Delta\varepsilon_{\alpha}^0(\tau) + \sum_j D_{ij}(t-\tau) \Delta\varepsilon_j^0(\tau) \right]. \quad (4.6)$$

Analogously, the increment $\Delta\varepsilon_i^L(t)$ is caused by the virtual distortion $\Delta\varepsilon_{\alpha}^0(t)$, modelling piezoelectric excitations, while the increment $\Delta\varepsilon_i^R(t)$ is caused by the defect-simulating virtual distortions $\Delta\varepsilon_j^0(t)$. Now, the following relation, between the defect parameters μ_i and the virtual distortion increment $\Delta\varepsilon_i^0(t)$ simulating this defect (in the time instance t), can be reached:

$$\sum_j [\delta_{ij} - (1 - \mu_i) D_{ij}(0)] \Delta\varepsilon_j^0(t) = (1 - \mu_i) \left[\sum_{\tau \leq t} \sum_{\alpha} D_{i\alpha}(t-\tau) \Delta\varepsilon_{\alpha}^0(\tau) + \sum_{\tau < t} \sum_j D_{ij}(t-\tau) \Delta\varepsilon_j^0(\tau) \right]. \quad (4.7)$$

Note that to achieve the above expression the following relation has been used:

$$\Delta\varepsilon_i^R(t) = \sum_{\tau \leq t} \sum_j D_{ij}(t-\tau) \Delta\varepsilon_j^0(\tau) = \sum_j D_{ij}(0) \Delta\varepsilon_j^0(t) + \sum_{\tau < t} \sum_j D_{ij}(t-\tau) \Delta\varepsilon_j^0(\tau). \quad (4.8)$$

For the distinguished time instant t , the formula (4.7) represents a set of i equations with $j = i$ unknowns $\Delta\varepsilon_j^0(t)$. To obtain $\Delta\varepsilon_j^0(t)$ for the entire time period $\langle 0, T \rangle$, we have to solve (step by step) the set (4.7) for all successive time instances $t \in \langle 0, T \rangle$. Knowing the defect parameters μ_i , the step by step (for the sequence of time instances t) determination of the increments $\Delta\varepsilon_i^0(t)$ can be performed. Then, knowing $\Delta\varepsilon_i^0(\tau)$ for $\tau \in \langle 0, t \rangle$, the strain increments in the observed location $\Delta\varepsilon_A(t)$ can be calculated making use of the equation (4.3). Summing these increments, like in the expression (4.2), we can determine the function of the strains $\varepsilon_A(t)$ in location A and the time period $\langle 0, T \rangle$.

4.1.3 Damage identification

Let us now formulate the inverse problem of damage identification requiring determination of the defect size and location (specified by the defect vector μ_i), knowing (from measurements) the functions of the strain response $\Delta\varepsilon_A^M(t)$ in locations A to the known excitation $\Delta\varepsilon_{\alpha}^0(\tau)$ generated in locations α . Therefore, the problem leads actually to the determination of the vector μ_i , where that assumed in advance locations i (potentially the whole structure) should allow for every possible distribution of defects. Assume for the

objective function f the sum of the following measures f_A of the distance between the observed response $\varepsilon_A^M(t)$ in location A and the appropriate possible response $\varepsilon_A(t)$, which depends on the defect-simulating virtual distortions $\Delta\varepsilon_j^0(t, \mu_i)$:

$$f = \sum_A f_A = \sum_A \sum_t [d_A(t)]^2, \quad (4.9)$$

where

$$\begin{aligned} d_A(t) &= \varepsilon_A^M(t) - \varepsilon_A(t) = \varepsilon_A^M(t) - [\varepsilon_A^L(t) + \varepsilon_A^R(t)] = \varepsilon_A^M(t) - \sum_t [\Delta\varepsilon_A^L(t) + \Delta\varepsilon_A^R(t)] = \\ &= \varepsilon_A^M(t) - \sum_{\tau \leq t} \sum_{\tau' \leq \tau} \left[\sum_{\alpha} D_{A\alpha}(\tau - \tau') \Delta\varepsilon_{\alpha}^0(\tau') + \sum_j D_{Aj}(\tau - \tau') \Delta\varepsilon_j^0(\tau', \mu_i) \right]. \end{aligned} \quad (4.10)$$

The most probable defect identification leads to the minimisation problem $\min f$, with respect to the control parameters μ_i . To this end, the gradient approach can be applied, with the following analytical gradient calculated from the formulae (4.9), (4.10):

$$\frac{\partial f}{\partial \mu_k} = \sum_A \frac{\partial f_A}{\partial \mu_k} = -2 \sum_A \sum_t d_A(t) \left[\sum_{\tau \leq t} \sum_{\tau' \leq \tau} \sum_j D_{Aj}(\tau - \tau') \frac{\partial \Delta\varepsilon_j^0(\tau', \mu_i)}{\partial \mu_k} \right], \quad (4.11)$$

where the partial derivatives $\partial \Delta\varepsilon_j^0 / \partial \mu_k$ can be determined from the following systems of equations obtained through differentiation of the formula (4.7):

$$\sum_j [\delta_{ij} - (1 - \mu_i) D_{ij}(0)] \frac{\partial \Delta\varepsilon_j^0(t, \mu_l)}{\partial \mu_k} = -\delta_{ik} \Delta\varepsilon_i(t) + (1 - \mu_i) \sum_{\tau < t} \sum_j D_{ij}(t - \tau) \frac{\partial \Delta\varepsilon_j^0(\tau, \mu_l)}{\partial \mu_k}. \quad (4.12)$$

Actually, for the distinguished time instant t , we have got here k sets of equations, where every set consists of i linear equations with j unknowns (and of course $i = j = k$). The iterative algorithm for the multi-defect identification requires calculation (from Eqs. (4.7) and (4.12)) of the defect-simulating distortion increments $\Delta\varepsilon_i^0(t)$ and their gradients $\partial \Delta\varepsilon_i^0 / \partial \mu_j$, for each time step of the dynamic analysis. Making use of these components, the objective function (4.9), (4.10) and its gradient (4.11) can be calculated. Having determined the gradient of the objective function, a modification of the material redistribution can be proposed:

$$\mu_i = \mu_i - \frac{\partial f}{\partial \mu_i} \Delta, \quad (4.13)$$

where the step length Δ can be adjusted e.g. due to the steepest descent optimisation strategy. Then, the calculation of the objective function and its gradient for the modified structure response can be performed in the next iteration. Alternatively, more advanced optimisation methods, e.g. conjugate gradient or variable metric, have been employed to look for the vector μ_j , which minimises the objective function (4.9).

5 Numerical example of a truss structure

5.1 Presentation of results

A 40-element cantilever truss structure, shown in Fig. 5.1, consisting of 8 repeatable 5 m x 5 m segments, has been analysed to test the DAMID code. All elements have the same tubular cross sectional area $A=201 \text{ cm}^2$ (65 cm diameter, 1 cm thickness) and Young's modulus $E=210 \text{ GPa}$. The structure was dynamically loaded with the sine excitation of the frequency $f=34.5 \text{ Hz}$, opposite in phase (cf. Fig. 4.1), which has been applied in elements Nos. 36 and 38, depicted in Fig. 5.1. The time of analysis has been set to $t=0.05\text{s}$ with 500 time steps assumed. Four analyses have been performed.

Analysis 1

At first, one defect was assumed in the element No. 13 with $\mu_{13}=0.2$, shown in Fig. 5.1. The member No. 1 was chosen as sensor, receiving the propagated wave. The corresponding elastic wave detected by the sensor and the wave generated in undamaged structure are shown in Fig. 5.2. The convergence of the identification process is depicted in Fig. 5.3. The number of potentially damaged elements chosen arbitrarily for lowest computational cost was reduced to just one.

Analysis 3

Another analysis was done for a structure with four defects - in the element No. 13 with $\mu_{13}=0.7$, the element No. 23 with $\mu_{23}=0.6$, the element No. 28 with $\mu_{28}=0.5$, the element No. 33 with $\mu_{33}=0.4$ - shown in Fig. 5.7. The strain wave detected by one sensor in element No. 1 is depicted in Fig. 5.8. The convergence of the identification process, achieved with 5 potentially damaged elements, is shown in Fig. 5.9.

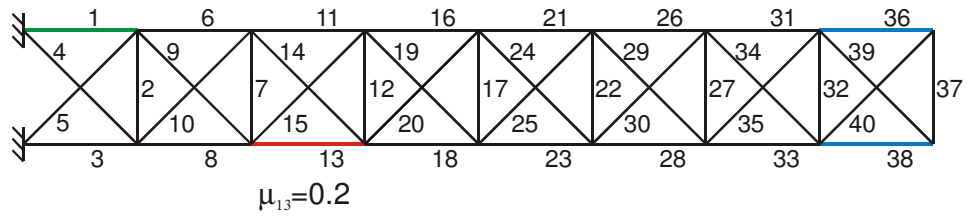


Fig. 5.1 One defect in dynamic identification

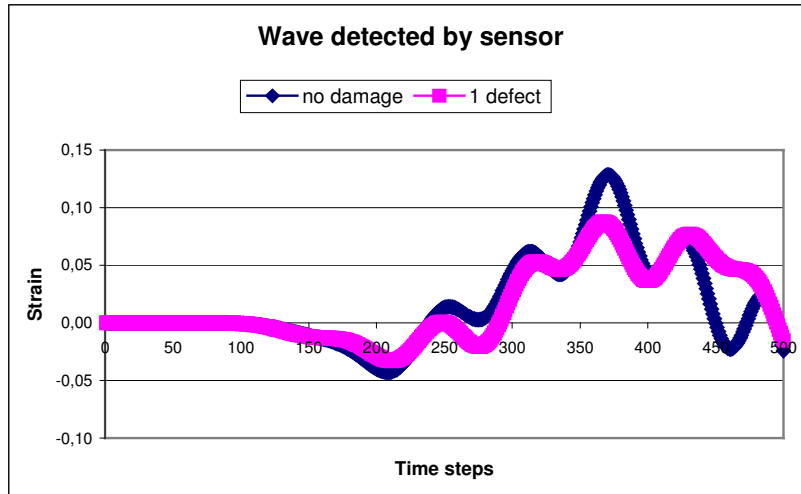


Fig. 5.2 Elastic wave detected by 1 sensor for 1 damage case

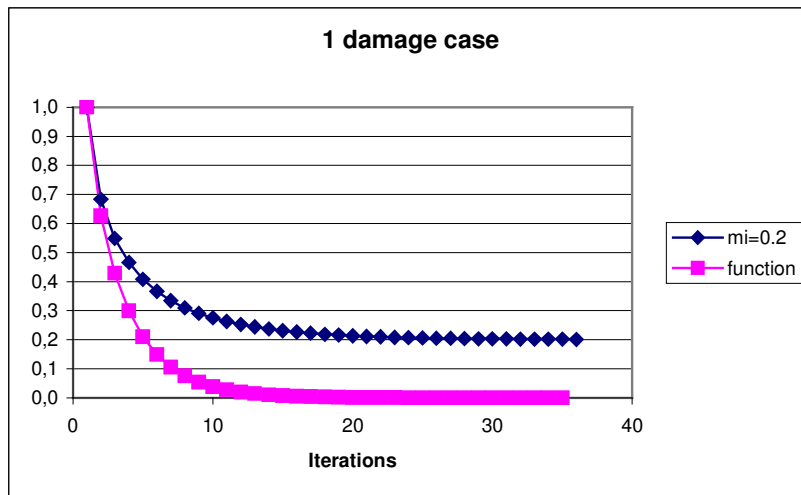


Fig. 5.3 Damage identification convergence for 1 damage case

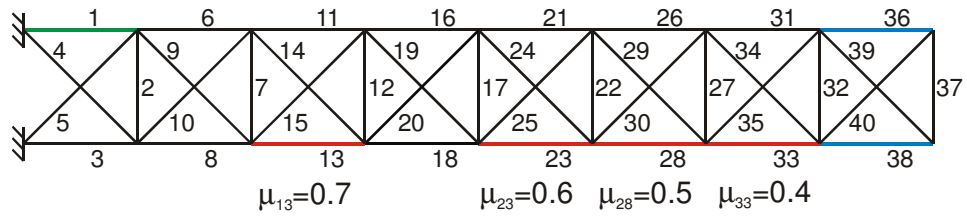


Fig. 5.7 Four defects in dynamic identification

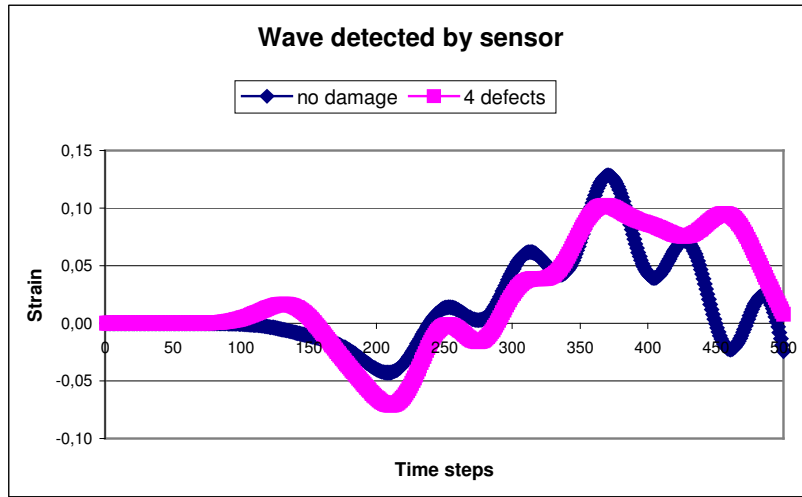


Fig. 5.8 Elastic wave detected by 1 sensor for 4 damage case

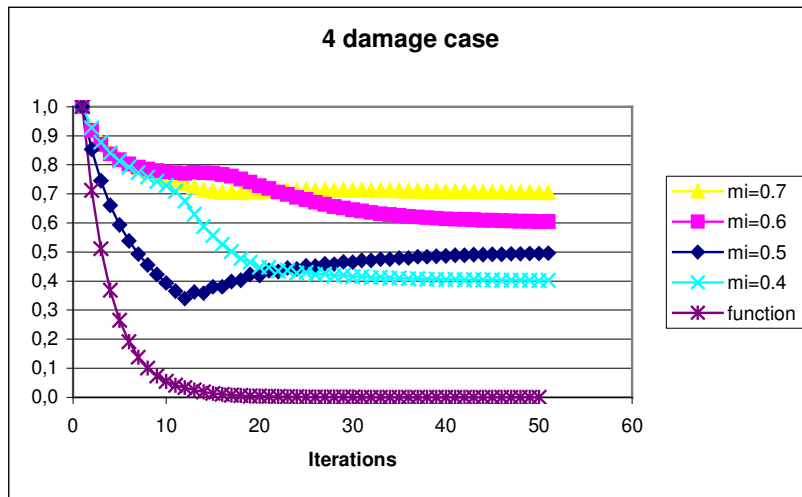


Fig. 5.9 Damage identification convergence for 4 damage case

6 Final remarks

6.1 General observations

The new concept of time-dependent VDM has proved to be effective in solution of the inverse dynamic problem. The objective function, analogous to the static case, is expressed in terms of time-dependent influence matrix and virtual distortions. Unlike the static case, the number and location of sensors is not the key issue in dynamics.

The major innovation of the proposed approach is successful application of the VDM to the solution of the inverse dynamic problem. The damage is modelled by the parameter μ (loss of stiffness) and the gradients of the objective function are calculated analytically. As a result the VDM-based software is very competitive in terms of effectiveness to other tools e.g. based on soft-computing methods. The authors are not aware of any other method than their own able to identify several simultaneous damage locations of different intensities by analysing the transient structural response.

At start of the VDM-based analysis, the influence matrix D must be numerically calculated and stored. For real engineering structures the cost of creating this matrix may be quite significant. Therefore any information on probable damage location would be precious as the analysis could be concentrated on some selected part of the structure only. The main cost of numerical analysis by the VDM-based software is computation of the objective function gradient, which is very costly due to the necessity of performing nested loops over the time and damaged members domain. However this cost was significantly reduced by introducing the idea of ranking all elements by initial gradient and contracting the space of potentially damaged elements from all members to an arbitrarily chosen number of members (usually small compared to all members).

The dynamic formulation of the VDM is a time-domain-based approach making use of data collected in many (e.g. 500) consecutive time steps and therefore capable of:

- modelling the propagation of elastic waves in structures,
- modelling damage in structural elements,
- solving the inverse dynamic problem of damage identification i.e. identifying multi-damage cases by comparing the undamaged and damaged structure responses.

6.2 Problems of numerical modelling

In numerical modelling of the VDM-based damage identification, the following problems must be taken into account and addressed appropriately:

- 1) FE discretisation – when we start dealing with continual models (e.g. the beam model) it is important to think of their discretisation in advance. Assuming too small elements will result in high numerical cost and assuming too large elements will make it impossible to detect small defects (smaller than the element used). So it is important to find a compromise for a numerical analysis between the computational cost involved and the required defect accuracy.

- 2) Setting dynamic analysis parameters – it is crucial to set the number of time steps in the Newmark’s integration so that it is a compromise between the identification accuracy that we need (the more steps the better) and the computation time we allow for (the less steps the better). We should also remember to set the time of the whole analysis in such a way that only the front of the wave is considered.
- 3) Optimal location of wave generators and sensors – when locating wave generators and sensors in the structure, engineering experience supported by experimental results may be utilised. There are such locations for actuators, which enable to generate a well-propagating strain wave, in the contrary to others. On the other hand if we have some hints on where to expect the damage we could make use of the information contained in the objective function gradients. By analysing the ranking of gradients for undamaged structure we can point out such sensor locations, which “prefer” damage in expected places.
- 4) Proper choice of the excitation frequency, close to some eigen-frequency but not affecting the stability of the system, providing long-distance propagation – when choosing the excitation for our model one should bear in mind that it affects the identification ability. High excitation frequency seems to be more adequate as it induces a wave of lower length, able to detect smaller defects. On the other hand, high-frequency-excited wave does not propagate well into long distances. So the choice of the excitation frequency is a compromise between the identification ability and the propagation ability of the induced wave.

6.3 Unsolved problems and future work

It is known that the inverse problems of damage identification involve many local minima. Achieving the global minimum (true location and intensity of damage) is hardly possible for real-life data. False damage locations are often observed. Therefore the VDM-based approach has been first tested with numerical (noise-free) data and did prove to find the damage locations and intensities assumed a priori. The effectiveness of the method for experimental data will be the subject of future research.

The accuracy of the multi-damage identification results, obtained through the VDM-based approach, presented in chapter 5, is high due to the fact that the measured response ε^M is noise-free i.e. generated numerically, not taken from experiment. The influence of noise is considered in the simple experiment described in chapter 3. The identification results for noisy data are not so accurate any more, but the damage location is indicated correctly, with some uncertainty (see Fig. 3.4). The uncertainty can be reduced by careful tuning of the numerical model to experimental data in order to achieve the most reliable response.

The sensitivity analysis of the method is the next challenge. Preliminary analysis has been done. In-depth investigation should include first of all the impact of measurement noise on identification results.

Acknowledgement

This work was financially supported by the grant No. KBN 5 T07A 052 22 awarded by the State Committee of Scientific Research, Warsaw, Poland and by the 5FP EU Growth Project No. G1RD-2001-00659 – PIEZODIAGNOSTICS – Smart Structural Diagnostics using Piezo-generated Elastic Waves.